Vol 15 No 7, July 2006
1009-1963/2006/15(07)/1481-05

Chinese Physics

© 2006 Chin. Phys. Soc.
and IOP Publishing Ltd

Isoscaling of projectile-like fragments*

Zhong Chen(钟 晨), Ma Yu-Gang(马余刚)†, Fang De-Qing(方德清), Cai Xiang-Zhou(蔡翔舟), Chen Jin-Gen(陈金根), Shen Wen-Qing(沈文庆), Tian Wen-Dong(田文栋), Wang Kun(王 鲲), Wei Yi-Bin(魏义彬), Chen Jin-Hui(陈金辉), Guo Wei(郭 威), Ma Chun-Wang(马春旺), Ma Guo-Liang(马国亮), Su Qian-Min(苏前敏), Yan Ting-Zhi(颜庭志), and Zuo Jia-Xu(左嘉旭)

Shanghai Institute of Applied Physics, Chinese Academy of Sciences, Shanghai 201800, *China*

(Received 30 November 2005; revised manuscript received 24 January 2006)

In this paper, the isotopic and isotonic distributions of projectile fragmentation products have been simulated by a modified statistical abrasion–ablation model and the isoscaling behaviour of projectile-like fragments has been discussed. The isoscaling parameters α and β have been extracted respectively, for hot fragments before evaporation and cold fragments after evaporation. It looks that the evaporation has stronger effect on α than β. For cold fragments, a monotonic increase of α and $|\beta|$ with the increase of Z and N is observed. The relation between isoscaling parameter and the change of isospin content is discussed.

Keywords: heavy ion reaction, projectile fragmentation, isoscaling
PACC: 2500, 2570N, 3130G

Recently, isoscaling behaviour has been extensively observed.[1−4] The scaling law relates ratios of isotope yields measured in two different nuclear reactions, 1 and 2, $R_{21}(N,Z) = Y_2(N,Z)/Y_1(N,Z)$. In multifragmentation events, such ratios are shown to obey an exponential dependence on the neutron number N or proton number Z of the isotopes characterized by three parameters α, β and C[1]:

$$R_{21}(N,Z) = \frac{Y_2(N,Z)}{Y_1(N,Z)} = C\exp(\alpha N + \beta Z). \qquad (1)$$

In the grand-canonical limit, $\alpha = \Delta\mu_{\rm n}/T$ and $\beta = \Delta\mu_{\rm z}/T$ where $\Delta\mu_{\rm n}$ and $\Delta\mu_{\rm z}$ are the differences between the neutron and proton chemical potentials for two reactions respectively. C is an overall normalization constant. This behaviour is attributed to the difference of isospin asymmetry between two reaction systems with similar nuclear temperature. It is potential to probe the isospin dependent nuclear equation of state[5,6] by the studies of isoscaling.[1−4,7,8] So far, the isoscaling behaviour has been studied experimentally and theoretically for different reaction mechanisms. However, most studies focus on the isoscaling behaviours for light particles. A few studies on the heavy projectile-like residues in deep elastic collisions and fission fragments have been reported.[9−13] In this paper, we concentrate our attentions on the isoscaling features in projectile fragmentation and discuss the effect of evaporation on the isoscaling parameters α and β in a framework of the statistical abrasion–ablation (SAA) model.[14]

Projectile fragmentation is one of the most important methods to produce beams of extreme neutron-rich or proton-rich nuclei and has been widely used to study nuclear reactions induced by heavy ions at intermediate and high energies. Various physical models for projectile fragmentation have been developed and the reaction mechanisms of heavy-ion collisions have been investigated extensively. For instance, an empirical parametrization, like EPAX/EPAX II formula presented by Sümmerer *et al*,[15,16] can predict the fragment production cross-section well. However, due to its poor physical foundation, the empirical parametrization may not be applicable in extrapolation. In addition, the SAA model can describe the isotopic distribution well.[14] In the SAA model, the nuclear reaction is described in two stages which occur in two distinctly different time scales. The first abrasion stage is fragmentation reaction which describes the production of the prefragment with certain amount excitation energy through the independent nucleon–nucleon collisions in the overlap zone of the colliding nuclei. The collisions are described by a picture of in-

*Project supported in part by the Shanghai Development Foundation for Science and Technology of China (Grant Nos 05XD14021 and 03QA14066), the National Natural Science Foundation of China (Grant Nos 10328259, 10135030, 10405032, 10405033 and 10475108), the Major State Basic Research Development Program of China (Contract No G200077404).
†Corresponding author. E-mail: ygma@sinap.ac.cn

teracting tubes. Assuming a binomial distribution for the absorbed projectile neutrons and protons in the interaction of a specific pair of tubes, we can determine the distributions of the total abraded neutrons and protons. For an infinitesimal tube in the projectile, the transmission probabilities for neutrons (protons) at a given impact parameter $\boldsymbol{b}$ are calculated by[14]

$$t_k(\boldsymbol{r}-\boldsymbol{b}) = \exp\{-[D_{\rm n}^{\rm T}(\boldsymbol{r}-\boldsymbol{b})\sigma_{\rm nk} + D_{\rm p}^{\rm T}(\boldsymbol{r}-\boldsymbol{b})\sigma_{\rm pk}]\}, \quad (2)$$

where $D^{\rm T}$ is thickness function of the target, which is normalized by

$$\int {\rm d}^2 r D_{\rm n}^{\rm T} = N^{\rm T}, \quad \int {\rm d}^2 r D_{\rm p}^{\rm T} = Z^{\rm T}$$

with $N^{\rm T}$ and $Z^{\rm T}$ referring to the neutron and proton number in the target respectively, the vectors $\boldsymbol{r}$ and $\boldsymbol{b}$ are defined in the plane perpendicular to beam, and $\sigma_{k'k}$ is the free nucleon–nucleon cross sections (k', k =n for neutron and k', k =p for proton). The thickness function of the target is given by

$$D_k^{\rm T}(\boldsymbol{r}) = \int_{-\infty}^{+\infty} {\rm d}\, z \rho_k((r^2+z^2)^{1/2}), \quad (3)$$

with ρ_k being the neutron (proton) density distribution of the target. So the average abraded mass at a given impact parameter $\boldsymbol{b}$ is calculated by the expression

$$\langle \Delta A(\boldsymbol{b})\rangle = \int {\rm d}^{\,2} r D_{\rm n}^{\rm P}(\boldsymbol{r})[1 - t_{\rm n}(\boldsymbol{r}-\boldsymbol{b})] + \int {\rm d}^{\,2} r D_{\rm p}^{\rm P}(\boldsymbol{r})[1 - t_{\rm p}(\boldsymbol{r}-\boldsymbol{b})]. \quad (4)$$

The excitation energy of projectile spectator is estimated by a simple relation of $E^* = 13.3\langle \Delta A(\boldsymbol{b})\rangle$ MeV where 13.3 is a mean excitation energy due to an abraded nucleon from the initial projectile.[17] In the second evaporation stage the system reorganizes due to excitation, which means that it is de-excited and thermalized by the cascade evaporation of light particles. By inducing the in-medium nucleon–nucleon cross section and optimizing the computational method proposed by our group given in Refs.[18–21], it can give a good agreement with the isotopic distribution at both high and intermediate energies involving neutron-rich or proton-rich nuclei over a wide energy range.[18,19,21] The isospin effect and its disappearance in projectile fragmentation for ^{36}Ar and ^{40}Ar at intermediate energies have been predicted by this model and confirmed by experimental data.[19]

In order to study the isoscaling effect in projectile fragmentation, the reactions of $^{40/36}$Ar + ^{9}Be at 60 MeV/nucleon were simulated by the SAA model. We extract the yield ratio $R_{21}(N,Z)$ by using the convention that index 2 refers to the more neutron-rich system (^{40}Ar + ^{9}Be) and index 1 refers to the less neutron-rich one (^{36}Ar + ^{9}Be). Figure 1 shows the yield ratios $R_{21}(N,Z)$ of hot projectile-like fragments (PLFs) as a function of neutron number N for selected isotopes (upper panel) and proton number Z for selected isotones (lower panel) for the $^{40/36}$Ar + ^{9}Be reactions in the semi-log plots. In Fig.2, the corresponding ratios for the cold PLFs are shown in the semi-log plots. In the figures, the different isotopes and isotones are shown by alternately filled and open symbols: even isotopes and isotones are shown with filled symbols while odd ones are shown with open symbols.

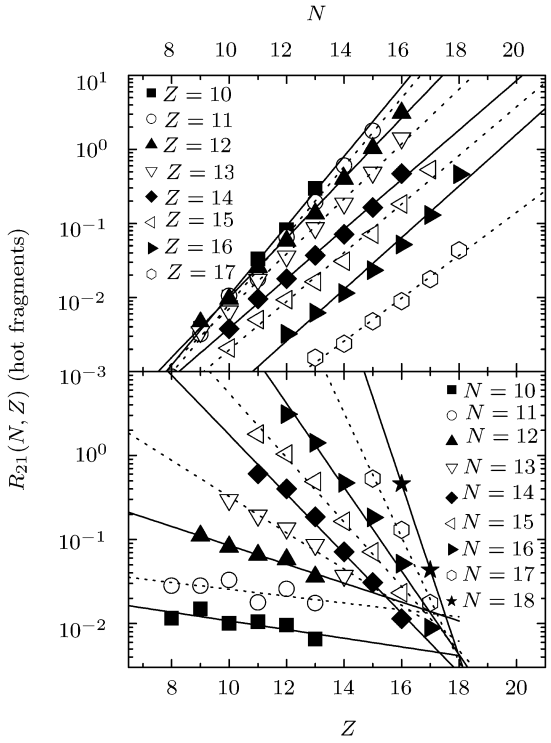


Fig.1. Yield ratios $R_{21}(N,Z)$ of pre-fragments (also called hot fragments in this work) from the reactions of ^{40}Ar + ^{9}Be and ^{36}Ar + ^{9}Be at 60 MeV/nucleon versus N (upper panel) or Z (lower panel). The lines represent the exponential fits.

From the upper panels of Fig.1 (hot fragments) and Fig.2 (cold fragments), we observe that the ratio for each isotope Z (from 10 to 17) exhibits a remarkable exponential behaviour. For each isotope (Z), an exponential function form $C\exp(\alpha N)$ was used to fit

the calculation points and the parameters α are shown in the top panel of Fig.3 for the selected Z. Analogous behaviour is observed in the lower panels of Figs.1 and 2, for each isotone (N), an exponential function form $C'\exp(\beta Z)$ was used to fit the calculation points and the parameters β are shown in the lower panel of Fig.3 for the selected N.

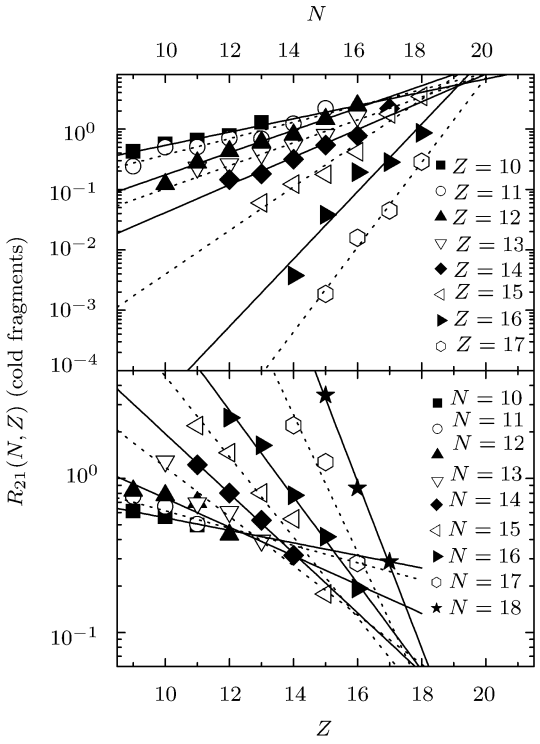


Fig.2. Yield ratios $R_{21}(N,Z)$ of cold fragments from the reactions of ^{40}Ar + ^{9}Be and ^{36}Ar + ^{9}Be at 60 MeV/nucleon versus N (upper panel) or Z (lower panel). The lines represent the exponential fits.

The model predicts that the fragment isotopic distribution at a fixed atomic number Z shifts towards the neutron-rich side for the neutron-rich projectile. In Fig.3, we present the slope parameters α (upper panel) and $|\beta|$ (lower panel) of the exponential fits obtained as described for Figs.1 and 2 as a function of Z and N respectively. In the upper panel of Fig.3, α of the pre-fragments for each element show a little bit decreasing trend with the increase of Z. But, a monotonic increase of $|\beta|$ with the increase of N is observed. For cold fragments which are survived after evaporation (open symbols of Fig.3), a monotonic increase of α and $|\beta|$ with the increase of Z and N respectively, is observed. Considering higher excitation for lower Z of projectile fragmentation, we know that the above behaviour for cold fragments indicates the facts that both α and β drop with the increase of excitation energy, or temperature.[19] This is consistent with many previous studies.[2,4,7] From the lower panel of Fig.3, $|\beta|$ always increase with the increase of N for hot fragments or cold fragments and $|\beta|$ of hot fragments tends to drop when evaporation is taken into account.

However, some cautions should be reminded. Since the first abrasion stage is essentially a fast geometrical abrasion stage, no equilibrium can be expected for the pre-fragments. These fragments are only intermediate stage products and will decay due to their excitation. In the strict sense, there is no isoscaling behaviour for this pre-fragments due to the lack of equilibrium. However, a similar analysis as the isoscaling can be done since there exists different isotopic/isotonic distributions between two systems. In this work, this kind of analysis is useful to investigate the evaporation effect on the isoscaling parameters of PLFs.[2]

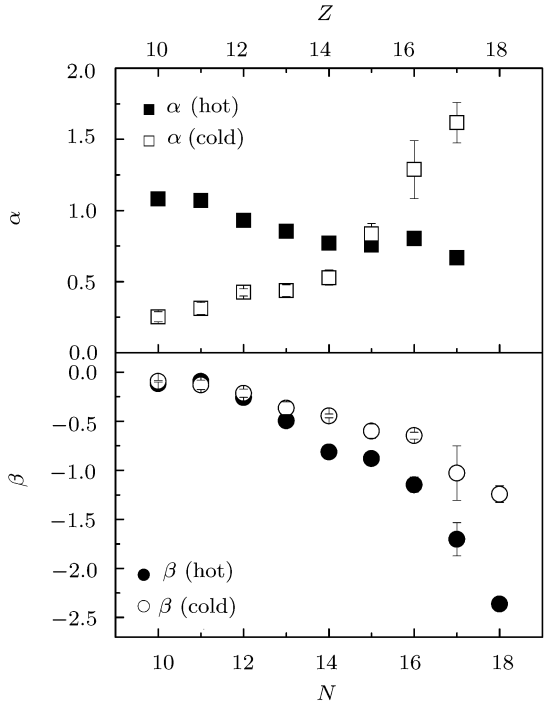


Fig.3. Isoscaling parameters α as a function of Z (upper panel) and β as a function of N (lower panel) for projectile fragmentation from the reactions ^{40}Ar+ ^{9}Be and ^{36}Ar+ ^{9}Be at 60 MeV/nucleon. Solid symbols represent the pre-fragments and open symbols represent final fragments.

In the evaporation stage, neutrons are emitted with the most important probability, the final cold fragments are more symmetric than their hot ancestors, which reflects a strong evaporation effect on

PLFs.[22,23] However, the charged particle emission is less important. Since α is the isoscaling parameter in fixed Z and β is the isoscaling parameter in fixed N, so the neutron evaporation has the strongest effect on α while charged particle evaporation has less effect on β. That results in an obvious change of α parameter while a weak change of β is due to the evaporation.

In order to further discuss the reason of the dramatic change of the isoscaling parameters, we plot $\langle N\rangle/Z$ versus Z in the upper panel of Fig.4 for the fragments before and after evaporation. As known, $\langle N\rangle/Z$ represents the isospin component. From the figure, the hot PLFs which are close to initial projectile basically remain larger isospin content as the initial projectile while lighter hot PLFs have much larger $\langle N\rangle/Z$ due to stronger dissipation and nucleon exchange. However, this high isospin content can not keep alive since the prefragments are excited as illustrated in the above section. They will cool themselves by the light particle evaporation, mostly by the neutron emission. After the evaporation process, $\langle N\rangle/Z$ tends to 1.1 in lower Z and bifurcates in higher Z for ^{40}Ar and ^{36}Ar systems. More interestingly, we note that the differences of $\langle N\rangle/Z$ between two systems for hot and cold fragments as a function of Z as shown in the lower panel of Fig.4. Consistently, this behaviour is similar to α as a function of Z for hot and cold PLFs as shown in Fig.3. In this context, we could say that the difference of isospin content (i.e. the neutron-to-proton ratio: $\langle N\rangle/Z$) is a more simple measurement of isoscaling behaviour. Similar behaviour has been found for $|\beta|$.

In the past years, the isospin dependence of various physical quantities has been reported.[5,19,24−29] The positive slopes in the upper panels of Figs.1 and 2 indicate that neutron-rich fragments are more efficiently produced, as expected, from the more neutron-rich systems. In other words, the fragment isotopic distribution at a fixed atomic number Z shifts towards the neutron rich side for the neutron-rich projectile. This isospin effect will decrease with the decrease of the fragment atomic number Z and disappear when $(Z_{\rm proj}-Z)/Z_{\rm proj}$ becomes larger.[19] The quantity of $(Z_{\rm proj}-Z)/Z_{\rm proj}$ can be related to excitation energy or temperature of the deformed projectile after the abrasion stage. When this quantity becomes smaller, the deformed projectile becomes hotter or highly excited. In this context, we can say that the isospin effect tends to fade out with the increase of the excitation energy of the projectile-like system.

In summary, the isoscaling of OLFs from $^{40/36}$Ar + ^{9}Be at 60 MeV/nucleon has been studied by a modified SAA model. SAA model can simulate well the isotopic distribution of PLFs of the systems. The isoscaling parameters α and β are extracted for the prefragments and final fragments. α has a dramatic change after evaporation. For hot PLFs, α shows a little bit stronger isospin effect for those highly excited small PLFs. However, this kind of stronger isospin effect for smaller PLFs cannot survive due to much more neutron evaporation from these highly excited pre-PLFs. Finally α shows weaker for these smaller PLFs while stronger for PLFs which are close to initial projectile. A monotonic increase of α ($|\beta|$) with the increase of Z (N) is observed, i.e. it indicates that both α and β drop with the increase of the excitation energy, or temperature. This behaviour can be easily explained by the difference of the isospin content of hot or cold PLFs between two systems as shown in Fig.4. In this sense, isospin content can take a simple 'isometre' as isoscaling parameter. In addition, the disappearance of the isospin effect of projectile fragmentation is also discussed from the viewpoint of the isoscaling parameter.

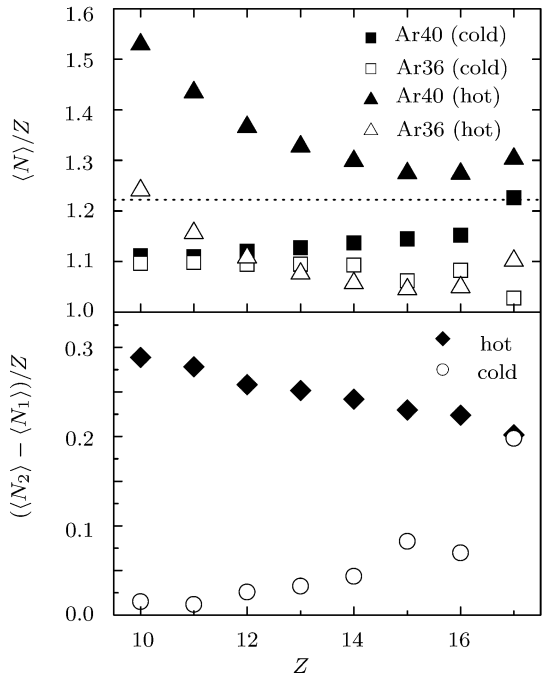


Fig.4. $\langle N\rangle/Z$ for hot and cold fragments for ^{40}Ar and ^{36}Ar systems. The dotted line is initial N/Z for ^{40}Ar (upper panel). The differences of $\langle N\rangle/Z$ between ^{40}Ar and ^{36}Ar are shown for the hot and cold fragments systems (lower panel). The symbols are illustrated in the insert.

References

[1] Tsang M B, Friedman W A, Gelbke C K, Lynch W G, Verde G and Xu H 2001 *Phys. Rev. Lett.* **86** 5023

[2] Tsang M B, Friedman W A, Gelbke C K, Lynch W G, Verde G and Xu H 2001 *Phys. Rev.* C **64** 041603

[3] Tsang M B, Gelbke C K, Liu X D, Lynch W G, Tan W P, Verde G, Xu H S, Friedman W A, Donangelo R, Souza S R, Das C B, Das Gupta S and Zhabinsky D 2001 *Phys. Rev.* C **64** 054615

[4] Botvina A S, Lozhkin O V and Trautmann W 2002 *Phys. Rev.* C **65** 044610

[5] Baran V, Colonna M, Greco V and Di Toro M 2005 *Phys. Rep.* **410** 335

[6] Ma Y G and Shen W Q 2004 *Nucl. Sci. Tech.* **15** 4

[7] Ma Y G, Wang K, Wei Y B, Ma G L, Cai X Z, Chen J G, Fang D Q, Guo W, Shen W Q, Tian W D and Zhong C 2004 *Phys. Rev.* C **69** 064610

[8] Tian W D, Ma Y G, Cai X Z, Chen J G, Chen J H, Fang D Q, Guo W, Ma C W, Ma G L, Shen W Q, Wang L, Wei Y B, Yan T Z, Zhong C and Zuo J X 2005 *Chin. Phys. Lett.* **22** 306

[9] Souliotis G A, Shetty D, Veselsky M, Chubarian G, Trache L, Keksis A, Martin E and Yennello S J 2003 *Phys. Rev.* C **68** 024605

[10] Friedman W A 2004 *Phys. Rev.* C **69** 031601(R)

[11] Veselsky M, Souliotis G A and Jandel M 2004 *Phys. Rev.* C **69** 044607

[12] Wang K, Ma Y G, Wei Y B, Cai X Z, Chen J G, Fang D Q, Guo W, Ma G L, Shen W Q, Tian W D, Zhong C and Zhou X F 2005 *Chin. Phys. Lett.* **22** 53

[13] Ma Y G, Wang K, Cai X Z, Chen J G, Chen J H, Fang D Q, Guo W, Ma C W, Ma G L, Shen W Q, Su Q M, Tian W D, Wei Y B, Yan T Z, Zhong C, Zhou X F and Zuo J X 2005 *Phys. Rev.* C **72** 064603

[14] Brohm T and Schmidt K H 1994 *Nucl. Phys.* A **569** 821

[15] Sümmerer K, Brüchle W, Morrissey D, Schädel M, Szweryn B and Yang W F 1990 *Phys. Rev.* C **42** 2546

[16] Sümmerer K and Blank B 1999 *Phys. Rev.* C **61** 34607

[17] Gimard J J and SchmidtK H 1991 *Nucl. Phys.* A **531** 109

[18] Fang D Q, Shen W Q, Feng J, Cai X Z, Wang J S, Su Q M, Ma Y G, Zhu Y T, Li S L, Wu H Y, Gou Q B, Jin G M, Zhan W L, Guo Z Y and Xiao G Q 2000 *Phys. Rev.* C **61** 044610

[19] Fang D Q, Shen W Q, Feng J, Cai X Z, Ma Y G, Zhang H Y, Hu P Y, Zhan W L, Guo Z Y, Xiao G Q, Li J X, Wang M, Wang J F, Ning Z J, Wang J Q, Wang J S, Wang Q J and Chen Z Q 2001 *Eur. Phys. J.* A **10** 381

[20] Cai X Z, Feng J, Shen W Q, Ma Y G, Wang J S and Ye W 1998 *Phys. Rev.* C **58** 572

[21] Zhong C, Fang D Q, Cai X Z, Shen W Q, Zhang H Y, Wei Y B and Ma Y G 2003 *High Energy Phys. Nucl.* (in Chinese) **27** 39

[22] Goldhaber A S 1974 *Phys. Lett.* B **53** 306

[23] Ma Y G, Wada R, Hagel K, Murray M, Wang J S, Qin L J, Makeev A, Smith P, Natowitz J B and Ono A 2002 *Phys. Rev.* C **65** 051602R

[24] Miller M L, Bjarki O, Magestro D J, Pak R, Stone N T B, Tonjes M B, Vander Molen A M, Westfall G D and Friedman W A 1999 *Phys. Rev. Lett.* **82** 1399

[25] Dempsey J F, Charity R J, Sobotka L G, Kunde G J, Gaff S, Gelbke C K, Glasmacher T, Huang M J, Lemmon R C, Lynch W G, Manduci L, Martin L, Tsang M B, Agnihotri D K, Djerroud M, Schröder W, Skulski W, Töke J and Friedman W A 1996 *Phys. Rev.* C **54** 1710

[26] Müller H and Serot B D 1995 *Phys. Rev.* C **52** 2072

[27] Ma Y G, Su Q M, Shen W Q, Han D D, Wang J S, Cai X Z, Fang D Q and Zhang H Y 1999 *Phys. Rev.* C **60** 024607

[28] Ma Y G, Su Q M, Shen W Q, Wang J S, Cai X Z and Fang D Q 1999 *Chin. Phys. Lett.* **16** 256

[29] Ma Y G 2000 *Acta Phys. Sci.* **49** 254 (in Chinese)